An All-Atomistic Molecular Dynamics Study to Determine the Structural Importance of Disulfide Bonds in Immunoglobulin G and Bovine Serum Albumin

Akshay Mathavan[a], Akash Mathavan[a], Michael E. Fortunato[b], & Coray M. Colina[bc]*

[a]Department of Biomedical Engineering, University of Florida, Gainesville, FL
[b]Department of Chemistry, University of Florida, Gainesville, FL
[c]Departments of Materials Science and Nuclear Engineering, University of Florida, Gainesville, FL

Students: amathavan1996@ufl.edu, amathavan2496@ufl.edu, mef231@chem.ufl.edu
*Mentor: colina@chem.ufl.edu**

ABSTRACT
A fully-atomistic molecular dynamics study was performed to determine the importance of disulfide bonds on the stability of immunoglobulin G (IgG) and bovine serum albumin (BSA). The transferability of a previous prescreening methodology to assess contributions from individual disulfide bonds on conformational stability was tested on both proteins. In IgG, it was apparent that inter-chain and intra-chain disulfide bonds play different roles in maintaining structure, evidenced by clear separation of inter-chain cysteine residues upon cleavage of disulfide bonds. In BSA, a set of double disulfide bonds required both to be broken in order to observe significant structural changes, equivalently seen in a previous study of human serum albumin (HSA), a structurally similar protein. Structural analysis of IgG showed deviations in distances between domains, while analysis of BSA suggested more local structural changes. This work helps confirm the efficacy and reproducibility of the prescreening methodology on both a novel, larger protein such as IgG and a more homologous (to HSA), globular protein such as BSA. The results provide insight into the role of specific disulfide bonds in the stability of IgG and BSA.

KEYWORDS
Molecular Dynamics; Atomistic Simulations; Immunoglobulin G; Bovine Serum Albumin; Disulfide Bonds

INTRODUCTION

Proteins are large molecules consisting of building-block units called amino acids. The linear sequence of amino acid residues for these biomolecules determines their three-dimensional structures. The complex assembly of multiple protein subunits can provide a vast array of functional capabilities ranging from enzyme catalysis to molecular transportation to antibody defense. Molecular flexibility introduced by regions of proteins lacking well defined structure can determine additional functional capacities; proteins with rigid components may serve as structural elements of a cell while those with flexible units may behave as hinges, springs, or levers.[1]

Disulfide bonds (SS bonds), covalent bonds between two cysteine residues, serve as important structural elements in proteins that ensure proper biological function. SS bonds establish conformational constraints on a peptide backbone, which can stabilize protein structure.[2] Native SS bonds maintain properly folded conformations and destabilize improper or denatured formations through a decrease of conformational entropy. Bowman-Birk inhibitor proteins possess exposed hydrophobic motifs, yet seven SS bonds lock their native conformation and provide stability against common denaturants.[3] Previous work has also emphasized the role of native SS bonds in determining the kinetics of folding pathways for proteins.[4] The stabilizing effect of SS bonds can also be seen in the increased melting point of proteins.

Protein aggregation, the accumulation of misfolded proteins, has often been correlated with cell toxicity and a variety of human diseases.[5–8] Protein aggregation in denaturing conditions has been suggested to result from the absence of native SS bonds.[3, 9, 10] In many extracellular native proteins, including antibodies, receptors, and hormones, almost all sulfhydryl groups form SS bonds.[3] SS bonds can form between residues within chains (intra-chain) or between chains (inter-chain) of proteins, and within domains (intra-domain) or between domains (inter-domain), with varied degrees of contribution towards structural stability.[10-13] In

denaturing environments, the presence of free cysteine residues in immunoglobulin G (IgG), an antibody, has been identified; the resulting lowered stability has been suggested to lead to non-native structures due to a high propensity for unfolding and aggregation.[11] Reduction of SS bonds in lysozymes and bovine serum albumin (BSA) has yielded the formation of amorphous non-native structures, leading to protein aggregates.[12]

While previous experimental studies have identified the importance of SS bonds on the maintenance of protein tertiary structure, atomistic molecular dynamics (MD) simulations offer an alternative method to study the effects of both native and non-native SS bonds on protein structure and stability at the molecular level.[13, 14] Previous MD simulations have studied the consequences of SS bond manipulation in signaling proteins, defense peptides, and biomarkers.[15–18] Atomistic simulations presented in this study employ a prescreening methodology introduced in previous work by our lab which served to identify potentially significant SS bonds in human serum albumin (HSA) by initially looking at protein structures with all native SS bonds removed, thereby avoiding the computational cost of a systematic approach.[19] Specifically, simulations of proteins with all native SS bonds removed were performed and separation distances between pairs of Sγ atoms of those cleaved SS bonds were computed. Notable deviations in separation distances hinted towards those SS bonds as being critical to maintaining local structure, and thus guided the investigation of these specific bonds as being potentially responsible for structural changes.

This work extends the procedure to study two other proteins, IgG and BSA. Although structurally distinct, both proteins possess significant numbers of SS bonds, which have been experimentally studied and shown to contribute to protein aggregation upon reduction or cleavage.[11–13] The large and flexible IgG protein presents a conformationally novel structure with which to apply the prescreening approach, and the significant structural homology between globular proteins BSA and HSA provides an opportunity to explore the relationship between protein structure and the role of SS bonds. Therefore, the purpose of this study was to apply the prescreening methodology, test its predictive capabilities, and understand the contributions of SS bonds at the atomistic level in two vastly different protein structures.

Immunoglobulins are large, Y-shaped glycoproteins. They are antibodies, major constituents of humoral immunity used to neutralize foreign toxins. IgG is the most abundant of five different immunoglobulins in humans (IgA, IgD, IgE, IgG, IgM). IgG itself can be further subdivided into four classes (IgG1, IgG2, IgG3, IgG4), of which IgG1 is the most prevalent serum antibody.[20] The structure of IgG1 is defined by three globular domains formed by the folding of two light chains (L and M), each 215 residues in length, and two heavy chains (H and K), each 457 residues in length. Two of the three domains contain peptide sequences that bind to antigens (F_{ab} domains) and the other domain (F_c domain) can bind to other proteins. These domains are linked by the hinge region, which imparts a range of motion and flexibility.[21] Although several structures of immunoglobulins have been published in the Protein Data Bank (PDB), only the 1HZH crystal structure captures the composition of human IgG1 antibodies.[22, 23] Due to the prevalence of IgG1 (hereafter simply referred to as IgG) in human serum as well as its recent applications to monoclonal antibody therapies, the 1HZH crystal structure was selected as the model molecule for this study.[24]

For the purposes of this work, the hinge of IgG was studied as an independent region; therefore, IgG consisted of the three domains and one region: $F_{ab}1$ (residues 1-230 of heavy chain H, 1-215 of light chain L), $F_{ab}2$ (residues 1-230 of heavy chain K, 1-215 of light chain M), F_c (residues 246-457 of heavy chain H and heavy chain K), and the hinge region (residues 231-245 of heavy chain H and heavy chain K). Residue numbers for IgG were defined with the relevant position and chain. IgG has 16 SS bonds, of which 12 are intra-chain and 4 are inter-chain. Two of the four inter-chain SS bonds are situated in the core hinge region, but experimental determination of the crystal structure for 1HZH showed that only one of the two pairs of cysteine residues were connected as SS bonds, indicating that the broken (unconnected) interchain SS bond may have been dynamic or a consequence of radiation damage.[23] However, the broken SS bond likely has no functional significance as previous work has shown that only a single hinge SS bond is necessary for immunoglobulin proteins to be biologically active.[25] **Figure 1** presents the structure and distribution of SS bonds in IgG, as well as the spatial arrangement of both the native connected and broken hinge SS bond.

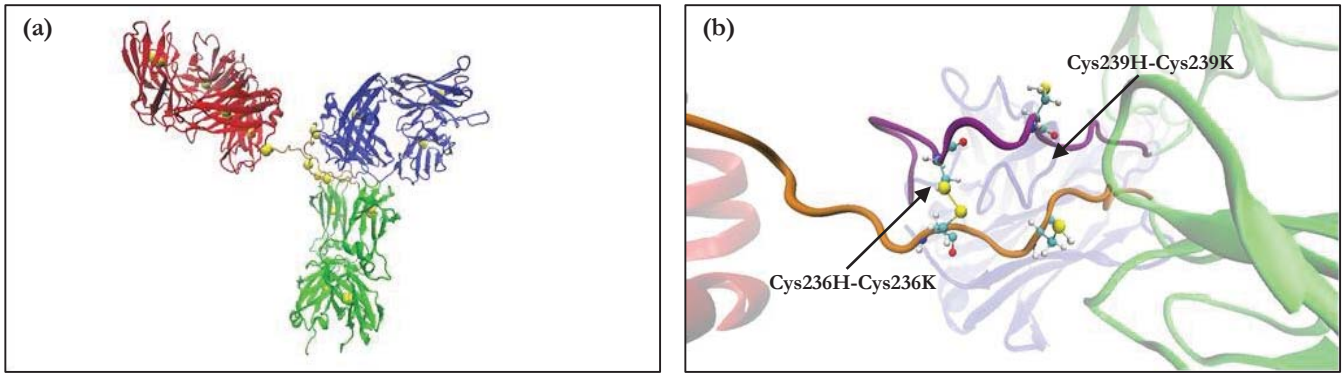

Figure 1. Cartoon representation of IgG (based on PDB entry 1HZH with homology modeling).[23] Regions (a) are represented as: $F_{ab}1$ (red), $F_{ab}2$ (blue), F_c (green), and hinge (orange). Sulfur atoms are depicted as yellow van der Waals (vdW) spheres. Chains of the hinge region (b) are represented as: residues 231H-245H (orange) and residues 231K-245K (purple). SS bonds are represented as ball-and-stick, with sulfur atoms as yellow. Connected (Cys236H-Cys236K) and broken (Cys239H-Cys239K) SS bonds are shown. The cartoons were created using Visual Molecular Dynamics.[26]

Serum albumins, the most prevalent circulatory proteins in mammals, function to preserve the body's osmotic pressure and are carrier proteins for compounds including hormones, fatty acids, and steroids. Serum albumins have been heavily studied due to their known primary and tertiary structures obtained through X-ray crystallography. They have also been the subject of significant drug delivery research, such as for applications in cancer drug therapy.[27] Bovine Serum Albumin (BSA) is a heart shaped serum albumin isolated from cows. It has a predominantly α (alpha) helix structure with 583 residues and 17 intradomain SS bonds.[28]

BSA was modeled in this study using PDB entry 3V03.[29] BSA consists of three homologous domains, which are each divided into two subdomains: IA (residues 1-105), IB (residues 106-193), IIA (residues 194-295), IIB (residues 296-381), IIIA (residues 382-494), and IIIB (residues 495-583). While specific subdomain residues were not listed for BSA, its close homology with HSA was used to match similar subdomain residues in BSA to HSA. Subdomain residue composition for HSA was obtained from PDB entry 1AO6.[30] The SS bonds in BSA are well distributed throughout the protein, with at least two SS bonds per subdomain. All SS bonds in BSA are intra-domain (within a domain). Of the 17 SS bonds, 16 form double SS bonds, which are adjacent (next to each other) SS bonds in the primary amino acid sequence. **Figure 2** presents the structure and SS bond distribution in BSA, as well as a double SS bond formed by Cys123-Cys168 and Cys167-Cys176.

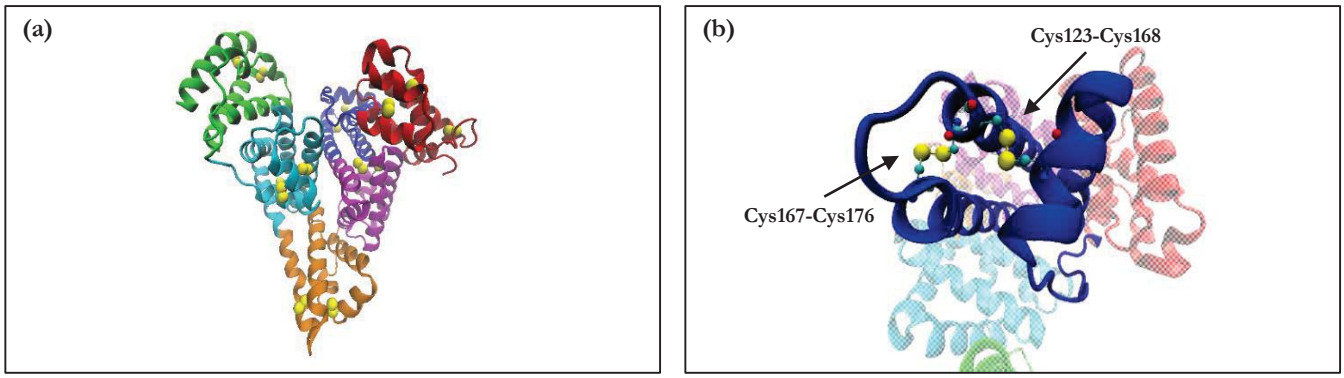

Figure 2. Cartoon representation of BSA (based on PDB entry 3V03).[29] Regions (a) are represented as subdomains: IA (red), IB (blue), IIA (purple), IIB (orange), IIIA (cyan), and IIIB (green). Sulfur atoms are depicted as yellow van der Waals (vdW) spheres. Double SS bond (b) formed by Cys123-Cys168 and Cys167-Cys176 is shown. SS bonds are represented as ball-and-stick, with sulfur atoms as yellow. The cartoons were created using Visual Molecular Dynamics.[26]

Due to the flexible nature of IgG, connected by a hinge region with no stabilizing secondary structure, it was hypothesized that inter-chain SS bonds (such as that found in the hinge region) would be important to structural stability. There is a similarity of structure between BSA and HSA, with SS bonds conserved across the albumin proteins. Therefore, it was hypothesized that homologous SS bonds in BSA would be more important for maintaining protein structure. This study reveals conformational changes in IgG and BSA when native SS bonds are removed. The prescreening methodology is applied to guide cleavage of specific SS bonds, and resulting systems are analyzed. This work provides a predictive tool, with utility in investigating phenomena such as protein aggregation.

METHODS AND PROCEDURES

Results for 1.6 μs of total simulation time using the AMBER16 simulation package are presented for IgG and BSA.[31] The SANDER program was used for energy optimization and the GPU-accelerated PMEMD program was used for production runs.[31, 32] Initial structures were generated from entries in the Protein Data Bank (PDB entries 1HZH and 3V03 for IgG and BSA, respectively) using LEaP and the Amber 14SB force field.[22, 23, 29, 33] Thirteen missing residues from heavy chain K in PDB crystal structure 1HZH were reconstructed using heavy chain H as a reference; the homology modeled 1HZH crystal structure is referred to as $1HZH^{+}$. For both proteins, the native disulfide (SS) bond connectivity was defined using information in the PDB entries. These disulfide bonds were those directly observed in experiment.[23, 29] Eight total simulations were performed with various SS bond connectivity for each protein. **Table 1** summarizes the cleavage of SS bonds in each MD simulation performed in this study. Non-zero charges were neutralized for each protein by adding counterions; 22 Cl^{-} and 16 Na^{+} ions were needed to neutralize IgG and BSA, respectively. Each protein was solvated with explicit TIP3P water in a truncated octahedral box with a buffering distance of 10 Angstroms (Å) and 20 Å for IgG and BSA, respectively, from the edge of the protein to any edge of the box.[34, 35]

Simulation Run	PDB	Protein	Length (ns)	Cleaved SS Bonds
1	$1HZH^{+}$	Immunoglobulin G	200	None
2	$1HZH^{+}$	Immunoglobulin G	200	All
3	$1HZH^{+}$	Immunoglobulin G	200	Cys236H-Cys236K (Hinge)
4	3V03	Bovine Serum Albumin	200	None
5	3V03	Bovine Serum Albumin	200	All
6	3V03	Bovine Serum Albumin	200	Cys123-Cys168
7	3V03	Bovine Serum Albumin	200	Cys167-Cys176
8	3V03	Bovine Serum Albumin	200	Cys123- Cys168 and Cys167-Cys176

Table 1. Summary of Molecular Dynamics simulations, detailing crystal structures, simulation lengths, and SS bond state for each run. Simulations were performed for a total time of 1.6 μs.

Energy minimization was conducted in two steps: 1) protein atoms were restrained to initial coordinates with a harmonic potential of 500.0 kCal/mol while the protein-water interface relaxed and 2) the whole system was relaxed with no restraints. Minimization consisted of steepest descent succeeded by conjugate gradient, each for an equal number of steps (total steps: 20000 for 1HZH and 25000 for BSA), with a 12 Å cutoff for all nonbonded interactions. The particle mesh Ewald algorithm was used to consider long range electrostatic interactions.[36-38] Then, each system was heated continuously from 0 to 300 K for a period of 40 ps, while protein atoms were restrained with a weak harmonic potential of 10.0 kCal/mol.

Heating of systems was followed by NPT (constant number of atoms, pressure, and temperature) simulations at 300 K, employing the Langevin thermostat and a collision frequency of 2.0 ps^{-1}. MD simulations were performed with periodic boundary conditions. The pressure was maintained at 1 atmosphere with a pressure relaxation time of 2 ps. The SHAKE Algorithm was applied during all MD simulations to place constraints on any bond containing hydrogen atoms. This permitted a time step of 2 fs, and system information was recorded every 20 ps. The CPPTRAJ module of AmberTools was used for analysis of the trajectories, including root mean squared deviation (RMSD), atomic distance and vector analysis.[31, 39]

RMSDs provided information about structural changes in the proteins. Atomic distances between sulfur atoms in pairs of cysteine residues were analyzed to identify the effects of SS bond cleavage on protein structure. Systems of each protein with all native SS bonds cleaved (simulation runs 2 and 5) were prepared and simulated. Separation distances between Sγ atoms were calculated and compared to equilibrium bond lengths. Following identification of Sγ atom pairs with noticeably large (>6 Å) separation distances, atomic simulations were performed with these specific SS bonds removed. Vector analysis and imaging in

Visual Molecular Dynamics (VMD) were used to investigate structural deviations with respect to changes in distances between domains of proteins.

RESULTS AND DISCUSSION

Root Mean Squared Deviation

Root mean square deviations (RMSDs) for backbone atoms (Cα, C, N) in IgG and BSA were calculated with reference to the initial crystal structures (in the case of IgG, 1HZH$^+$ was referenced). RMSDs measure average distances between atoms of a protein and reference structure throughout a simulation trajectory, providing information about possible conformational changes. These calculations were conducted for IgG structures in simulation runs 1, 2 and 3 (with SS Bonds, without SS Bonds, and without Cys236H-Cys236K, respectively) described in **Table 1**.

Results of RMSD calculations are presented in **Figure 3**. In all simulations, an increase in RMSD values was observed during the first ~20 ns, which can be attributed to the change in environment from X-ray crystallographic conditions to a solvated ambient environment. After ~30 ns, RMSD values in simulation run 1 fluctuated around an average of 7 Å. RMSD values in simulation run 2 increased for ~100 ns, after which values fluctuated around an average of 8 Å. The RMSD values for simulation run 3 increased initially (from a change to solvated environment), and increased again after ~60 ns. After ~120 ns, RMSD values fluctuated around an average of 10 Å. **Table 2** details RMSD information for simulation runs when no noticeable increase in RMSD values were observed (after ~30, ~100, and ~120 ns for simulation runs 1, 2, and 3, respectively).

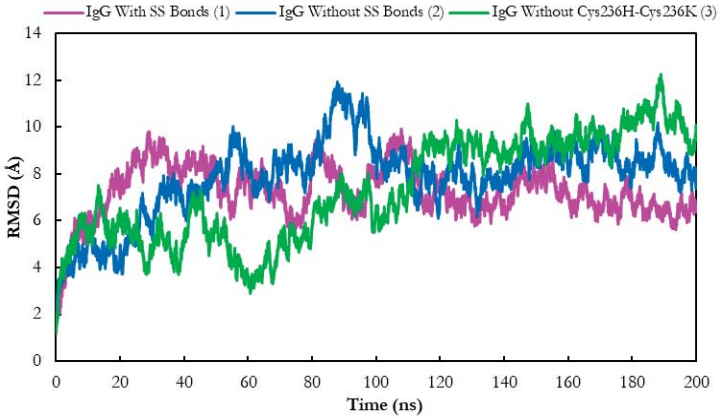

Figure 3. RMSDs for three cases of IgG simulations studied in this work, showing evolution over 200 ns for structures of IgG with SS Bonds (simulation run 1, in pink), without SS Bonds (simulation run 2, in blue), and without Cys236H-Cys236K (simulation run 3, in green), referencing crystal structure 1HZH$^+$.

Simulation Run	Average (Å)	Standard Deviation (Å)
1	6.9	0.6
2	8.4	0.6
3	9.6	0.7

Table 2. RMSDs for IgG simulations after no noticeable increases in values occurred. Provided are average and standard deviation of values for structures of IgG with SS Bonds (simulation run 1), without SS Bonds (simulation run 2), and without Cys236H-Cys236K (simulation run 3), referencing crystal structure 1HZH$^+$.

For simulation runs 1 and 2, RMSDs were also calculated for each domain of IgG. **Figure 4** presents the calculated RMSDs for each domain in simulation runs 1 and 2. In $F_{ab}1$, $F_{ab}2$, and F_c, RMSD values for both simulation runs initially increased and then fluctuated around an average of 1 to 3 Å. In the hinge region, RMSDs increased and fluctuated around ~5 and ~4 Å for simulation runs 1 and 2, respectively. Domain RMSD values were relatively smaller than those for the whole protein, agreeing with previous work that analyzed the protein structure of IgG.[40]

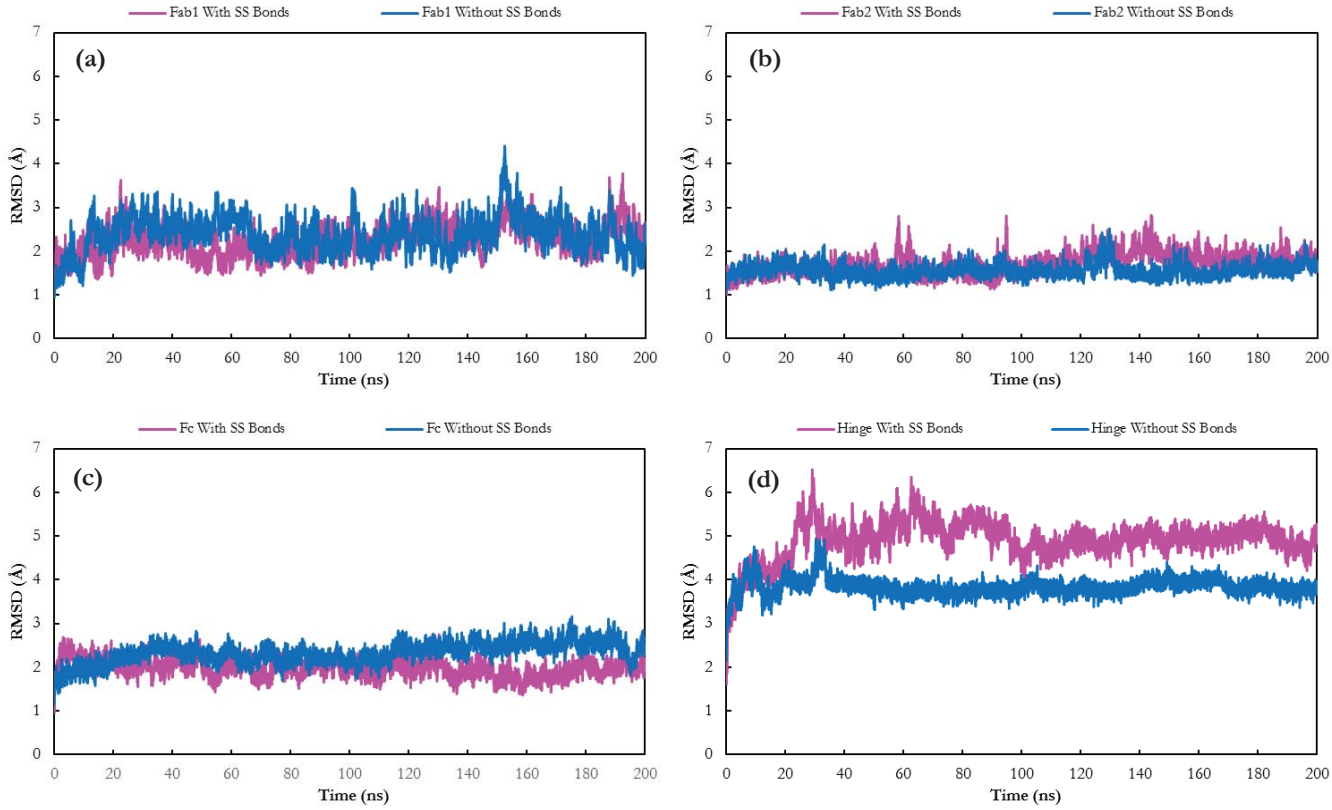

Figure 4. IgG domain RMSDs for backbone atoms during simulation runs 1 and 2 for: (a) $F_{ab}1$ domain, (b) $F_{ab}2$ domain, (c) F_c domain, and (d) hinge region. Results are presented for IgG with SS Bonds (simulation run 1, in pink) and without SS Bonds (simulation run 2, in blue), referencing crystal structure 1HZH+.

The RMSD analyses for IgG structures, shown in **Table 2,** provided information about the relative stability of the protein and possible conformational changes that occurred over 200 ns. Average RMSD calculations shown in **Figure 3** showed that values for the entire IgG backbone were noticeably higher (compared to domain RMSDs) than what would be expected for proteins in solvated conditions. Generally, larger collections of residues (as with the domains) would show larger backbone deviations. RMSD values for each domain of IgG, in **Figure 4**, were stable and lower than those of the whole protein, confirming the stability of the protein domains in solution and indicating that the relative motions of the domains contributed to the high average RMSD of the entire protein backbone structure. It was also evident that the hinge region, which contains a low number of residues, displayed higher backbone deviations in comparison to other domains. These results agree with well-studied segmental motion in IgG, in which the hinge region is known to impart a high degree of molecular flexibility.[21] Although RMSD values for all three IgG simulations reached a similar range of 6 to 10 Å, an increased equilibration time for simulation runs with non-native SS bond connectivity was observed. These longer equilibration timescales indicate that structural changes likely occurred.

RMSD calculations were also performed for BSA structures in simulation runs 4, 5, 6, 7, and 8, described in **Table 1**. Results for all simulation runs are shown in **Figure 5**. In all cases, an increase in RMSD values was seen during the first ~10 ns due to the change to a solvated environment. After ~10 ns, no noticeable deviation in RMSD was observed for all BSA simulation runs; with values fluctuating between 2 to 4 Å. **Table 3** presents average RMSD values for simulation runs 4-8 after ~10 ns.

Figure 5 shows that BSA RMSD values for all simulation runs (4-8) increased for only ~10 ns before equilibrating for the remainder of simulation time. When compared to IgG, the RMSDs showed relatively quick equilibration times and lower average values. This can be attributed to the globular nature of BSA, imposing a relative inflexibility. The results from the RMSD analysis did not indicate large scale structural changes even when cleaving SS bonds in BSA; however, that did not rule out possible changes to local protein structure which could play a role in ligand binding. Analysis of HSA, a structurally homologous protein, from previous work by our lab showed comparable RMSD values, with a range of 2 to 4 Å in corresponding simulations.[19]

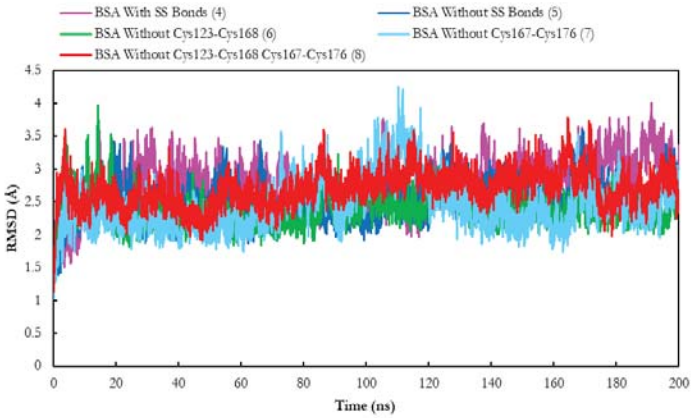

Figure 5. RMSDs for all runs of BSA simulations studied, showing evolution over 200 ns for structures of BSA with SS Bonds (simulation run 4, in pink), without SS Bonds (simulation run 5, in blue), without Cys123-Cys168 (simulation run 6, in green), without Cys167-Cys176 (simulation run 7, in teal), and without Cys123-Cys168 and Cys167-Cys176 (simulation run 8, in red), referencing crystal structure 3V03.

Simulation Run	Average (Å)	Standard Deviation (Å)
4	2.8	0.4
5	2.5	0.3
6	2.3	0.2
7	2.4	0.4
8	2.6	0.3

Table 3. RMSD values for simulations of BSA after 10 ns. Provided are average and standard deviation of values for structures of BSA with SS Bonds (simulation run 4), without SS Bonds (simulation run 5), without Cys123-Cys168 (simulation run 6), without Cys167-Cys176 (simulation run 7), and without Cys123-Cys168 and Cys167-Cys176 (simulation run 8), referencing crystal structure 3V03.

Disulfide Bonds

Analyses of separation distances for simulation runs 1, 2, 4, and 5 in **Table 1** (IgG and BSA with and without native SS bonds) provided information about SS bonds in both protein structures. SS bonds can be very important in maintaining protein structure; however, intermolecular interactions such as hydrogen bonding or the exclusion of water from hydrophobic regions can also help maintain protein structure. Analysis of experimental data have shown that in native, bonded states, sulfur atoms in pairs of cysteine residues maintain an average distance of 2.05 Å, with a standard deviation of 0.11 Å.[41] In the Amber 14SB force field, sulfur atoms in SS bonds are held together with a harmonic potential at an equilibrium bond distance of 2.038 Å. This enforces a narrow distribution of bond distances centered at this value in our simulations for sulfurs connected in SS bonds. Once SS bonds are broken, sulfur atoms interact through a Leonard Jones potential with a minimum in the energy well at a value of 4.00 Å. Consequently, most cleaved pairs of Sγ atoms maintain a range between 4 to 5 Å, suggesting that the Sγ atoms remain in close enough proximity to possibly reform the SS bond in the case it is broken. Therefore, it was not surprising to observe an increase in the separation distance of Sγ atoms to the range of 4 to 5 Å upon cleavage, as seen in the majority of distances for both IgG and BSA.

It is important to note, however, that the atomistic simulations presented here do not allow reformation of covalent bonds. Pairs of sulfur atoms that separate significantly upon cleavage of the SS bond have a much lower probability of bond reformation. Because Sγ atoms of cleaved SS bonds maintain an average distance of 4.1±0.5 Å, a significant separation was defined as >6 Å (roughly 4 standard deviations).[19] Thus, in the atomistic simulations, when the separation distance of Sγ atoms increased past 6 Å it was likely that there was not sufficient intermolecular interaction energy and it was probable that the SS bond existed to maintain local protein structure. In contrast, when pairs of Sγ atoms remained in close proximity after breaking a SS bond, the importance the SS bond played in maintaining local structure may have been supplemented with other protein-protein interactions. In each protein, separation distances between Sγ atoms of SS bonds were calculated. Separation distances in simulation runs with all native SS bonds connected were compared to distances in simulations runs with all native SS bonds

disconnected. As with native non-bonded cysteine residues, Sγ atoms in cysteine residues of proteins with no SS bonds were changed to a sulfhydryl group.

In IgG, separation distances for all connected SS bonds (simulation run 1) maintained an average value of 2.0 Å, with a standard deviation less than 0.1 Å. In IgG without native SS bonds (simulation run 2), distances between all pairs of Sγ atoms from cleaved intra-chain SS bonds ranged between 3 to 5 Å, with an average value of 3.8±0.3 Å. Given the Leonard Jones potential, this suggested possibility of bond reformation. In contrast, distances between pairs of Sγ atoms from cleaved inter-chain SS bonds were significantly higher, averaging 14.2±3.4 Å. **Table 4** details separation distances for Sγ atoms in IgG simulation run 2 (without SS bonds) for all 15 sulfhydryl pairs. **Figure 6** presents the separation distance between Sγ atoms for Cys236H-Cys236K, an inter-chain SS bond of the hinge region, in IgG simulation run 1 (with SS bonds) and simulation run 2 (without SS bonds). Separation distances in the remaining two inter-chain SS bonds (Cys230H-Cys215L and Cys230K-Cys215M) for simulation run 2 are also shown. Additionally, the separation distance between Sγ atoms of simulation run 2 for Cys22H-Cys96H, an intra-chain SS bond in $F_{ab}1$, is presented for comparison.

It is important to note that all intra-chain SS bonds in the protein with native SS bonds cleaved maintained a narrow separation distance distribution centered at 3.8 Å, indicating a possibility to reform the SS bond (see **Table 4**). Therefore, Cys22H-Cys96H was selected as a representative of intra-chain SS bonds to serve as a comparison in **Figure 6.** Similarly, all Sγ pair atom distances in IgG with SS bonds maintained a narrow separation distribution centered at 2.0 Å; therefore, Cys236H-Cys236K was selected to represent a bonded Sγ pair for comparison in **Figure 6**. As expected, distances between Sγ atoms of Cys236H-Cys236K in IgG simulation run 1 (with SS bonds) maintained an average separation distance of 2.0 Å. In IgG simulation run 2 (without SS bonds), distances between Sγ atoms of Cys22H-Cys96H averaged 3.8 Å. Separation distances for Sγ atoms of Cys236H-Cys236K were significantly higher, averaging at a value of 10.3 Å.

Sulfhydryl Pair	Inter-Chain SS Bond	Average (Å)	Standard deviation (Å)
22H-96H	No	3.8	0.3
23L-89L	No	3.9	0.3
154H-210H	No	3.9	0.4
135L-195L	No	3.8	0.4
22K-96K	No	3.8	0.3
23M-89M	No	3.9	0.3
154K-210K	No	3.8	0.3
135M-195M	No	3.8	0.4
271H-331H	No	3.9	0.4
377H-435H	No	3.8	0.4
271K-331K	No	3.9	0.3
377K-435K	No	3.8	0.3
230H-215L	Yes	16.4	1.7
230K-215M	Yes	15.8	2.6
236H-236K	Yes	10.3	0.9

Table 4. Summary of separation distances between Sγ atoms of all 15 sulfhydryl pairs of IgG without SS bonds (simulation run 2), including identification of inter-chain or intra-chain SS bonds. All intra-chain Sγ atoms maintained a distance suggestive of possible bond reformation (3 to 5 Å), while inter-chain Sγ atoms deviated significantly.

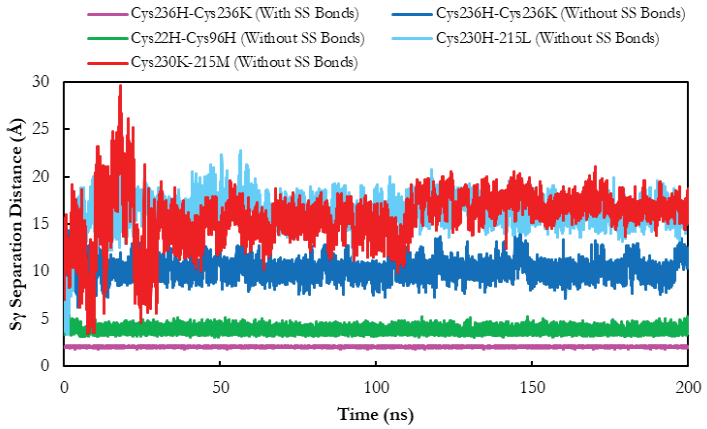

Figure 6. Separation distances between Sγ atoms of selected sulfhydryl pairs for IgG with SS Bonds (simulation run 1) and without SS Bonds (simulation run 2). Separation distances are presented for Cys236H-Cys236K with SS Bonds (simulation run 1, in pink), Cys236H-Cys236K without SS Bonds (simulation run 2, in blue), Cys22H-Cys96H without SS Bonds (simulation run 2, in green), Cys230H-Cys215L without SS bonds (simulation run 2, in teal) and Cys230K-Cys215M without SS bonds (simulation run 2, in red).

As discussed, Sγ atoms of intra-chain SS bonds in IgG without SS bonds sampled distances ranging between 3 to 5 Å. The previously developed prescreening methodology yielded three inter-chain Sγ atom pairs with significant distance separations. In addition to notable separation distances in the hinge Cys236H-Cys236K bond, the two remaining inter-chain SS bonds also deviated significantly (>6 Å). Cys230H-Cys215L and Cys230K-Cys215M are found at symmetric junctions of a heavy chain and light chain in $F_{ab}1$ and $F_{ab}2$, respectively, of IgG. Because intra-chain SS bonds of IgG are buried in a stable secondary structure of β (beta) sheets, it is hypothesized that cleaved bonds were supplemented by other local interactions. In inter-chain SS bonds, the large variability (range of 3 to 30 Å) and significantly increased values of Sγ atom separation distances suggested these SS bonds maintain local protein structure and possibly control the dynamic movement of F_{ab} domains. Previous work detailing the segmental motion and high degree of flexibility imparted by the hinge region, and therefore suggesting structural importance, prompted selection of Cys236H-Cys236K for cleavage.

Sγ atom pair separation distances were also calculated for BSA. Similar to IgG, Sγ atom pairs of BSA with native SS bonds connected maintained an average distance of 2.0 Å, with a standard deviation less than 0.1 Å, while most Sγ atom pairs in BSA with all native SS bonds disconnected sampled a range of distances from 3 to 5 Å, with an average value of 4.5±0.6 Å. Distances between Sγ atom pairs of Cys167-Cys176 and Cys123-Cys168 deviated significantly (>6 Å), averaging 7.0±2 Å and 5.0±1.5 Å, respectively. Sγ atom pairs of Cys475-Cys486, Cys513-Cys558, and Cys315-Cys360 also showed significant separation distances, fluctuating between 3 to 11 Å. Cys167-Cys176, comprised of a sulfhydryl pair with a noticeably high Sγ separation distance and a large degree of fluctuation, is part of a double SS bond with Cys123-Cys168. From the results of the prescreening approach, as well as a homologous double SS bond with high Sγ separation found in our previous study of HSA, this double SS bond was selected. Therefore, simulation runs 6-8 consisted of the native BSA structure with Cys123-Cys168 disconnected, Cys167-Cys176 disconnected, and both Cys123-Cys168 and Cys167-Cys176 disconnected, respectively.

Figure 7 presents a comparison between Sγ atom pair separation distances in Cys167-Cys176 in BSA with SS bonds (simulation run 4) and without SS bonds (simulation run 5). Additionally, Sγ atom pair separation distances in Cys199-Cys245 in BSA without SS bonds (simulation run 5) is presented. All Sγ atom pairs with no significant (<6 Å) separation distances maintained a narrow separation distance distribution centered at 4.5 Å, indicating a strong possibility of bond reformation given the Leonard Jones potential. Therefore, Cys199-Cys245 was selected to represent these SS bonds to serve as a comparison in **Figure 7**. Similarly, all Sγ pair atom distances in BSA with SS bonds maintained a narrow distance distribution centered at 2.0 Å; therefore, Cys167-Cys176 was selected as a bonded Sγ pair for comparison in **Figure 7**. As expected, distances between Sγ atoms of Cys167-Cys176 in BSA simulation run 4 (with SS bonds) maintained an average separation distance of 2.0 Å. In BSA simulation run 5 (without SS bonds), distances between Sγ atoms of Cys199-Cys245 averaged 4.9 Å. While separation distances exceeded 6 Å in several frames of the trajectory, Sγ atoms of Cys199-Cys245 remained in a separation range of 4 to 6 Å for the vast majority of simulation time, supporting the possibility of bond reformation. Sγ atoms of Cys167-Cys176 averaged a noticeably higher average value of 7.3 Å and sampled a range of distances from 4 to 13 Å.

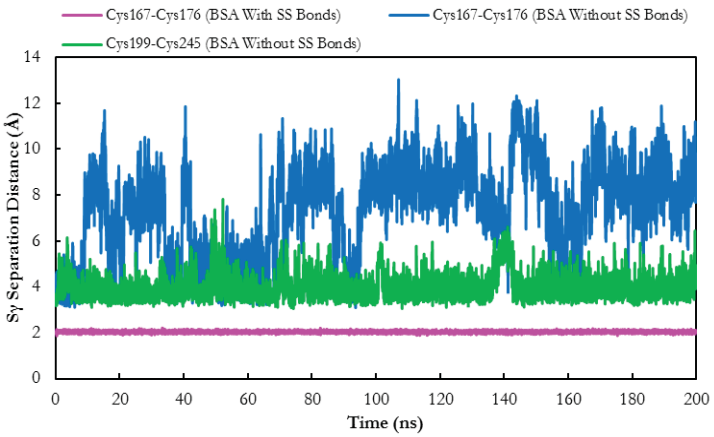

Figure 7. Separation distances between Sγ atoms of selected sulfhydryl pairs for BSA with SS Bonds (simulation run 4) and without SS Bonds (simulation run 5). Separation distances are presented for Cys167-Cys176 with SS Bonds (simulation run 4, in pink), Cys167-Cys176 without SS Bonds (simulation run 5, in blue), and Cys199-Cys245 without SS Bonds (simulation run 5, in green).

Figure 8a shows separation distances between Sγ atoms in Cys123-Cys168 for simulation runs 4 (with SS bonds), 6 (Cys123-Cys168 disconnected), and 8 (both Cys123-Cys168 and Cys167-176 disconnected). In simulation runs 6 and 8, Sγ atoms of Cys123-Cys168 maintained a similar separation distance, ranging between 4.5 to 6 Å. **Figure 8b** shows separation distance of Sγ atoms in Cys167-Cys176 for simulation runs 4 (with SS bonds), 7 (Cys167-Cys176 disconnected) and 8 (both Cys123-Cys168 and Cys167-176 disconnected). In contrast to Cys123-Cys168 Sγ atoms, Cys167-Cys176 Sγ atoms were able to separate to a greater extent when both Cys123-Cys168 and Cys167-Cys176 were broken in the double SS bond, as evidenced in a greater average separation distance of 8 Å in simulation run 8 compared to a distance of 5 Å in simulation run 7. **Figure 9** summarizes the average separation distances of Sγ atoms in Cys123-Cys168 and Cys167-Cys176 when only one or both of the double SS bonds were broken. The average separation distance of Cys167-Cys176 shown in **Figure 9** was calculated from data gathered after 100 ns, where clear separation was first observed.

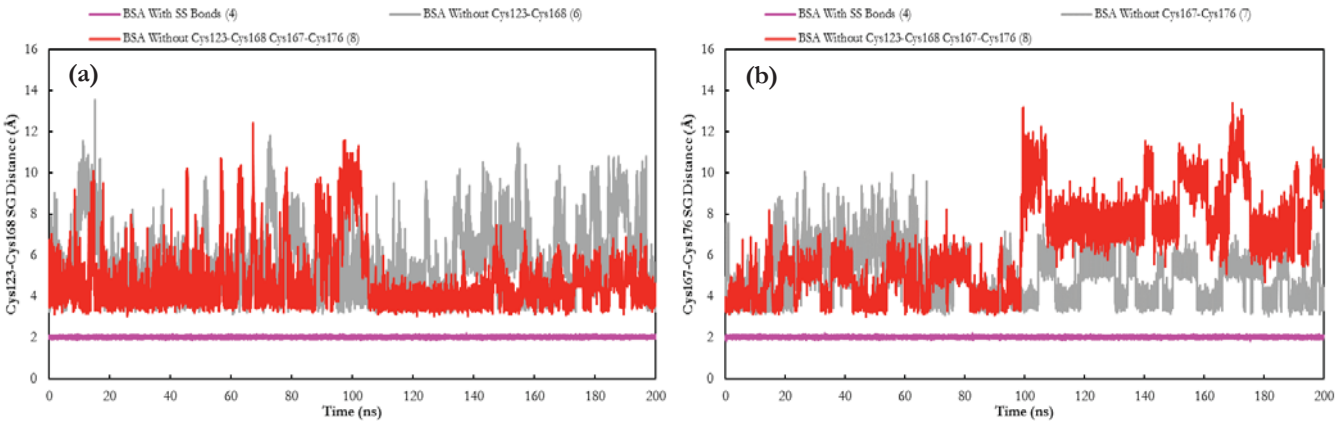

Figure 8. Separation distances between Sγ atoms of Cys123-Cys168 (a) and Cys167-Cys176 (b) for BSA simulation runs 4, 6, 7, and 8. Separation distances are presented for BSA with SS Bonds (simulation run 4, in pink), BSA without one SS Bond (simulation runs 6 and 7, in gray), and BSA without both SS Bonds (simulation run 8, in red).

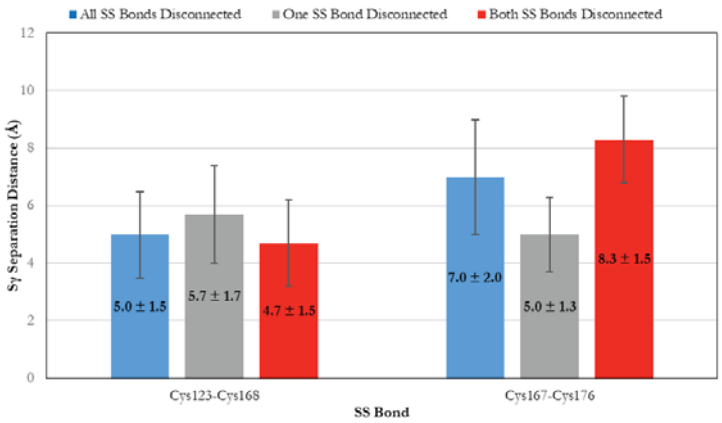

Figure 9. Summary of separation distances between Sγ atoms of Cys123-Cys168 and Cys167-Cys176 for BSA simulation runs 5-8. Separation distances are presented for BSA without SS Bonds (simulation run 5, in blue), BSA without one SS Bond (simulation runs 6 and 7, in gray), and BSA without both SS Bonds (simulation run 8, in red).

All 17 SS bonds in BSA are intra-domain and buried in the α helices of the protein structure. Results shown in **Figures 7-9** show that Cys123-Cys168 and Cys167-Cys176 form a double SS bond, in subdomain IB, with significant separation distances in Sγ atoms upon cleavage, suggesting contributions to protein structure stability. Lower separation distances in Sγ atoms of Cys123-Cys168 in comparison to Cys167-Cys176 also suggests that intermolecular forces may have contributed more to local protein structure stabilization around Cys123-Cys168, while Cys167-Cys176 may have been responsible in maintaining secondary or tertiary structure of BSA. Homologous SS bonds were identified in previous work on HSA, in which Cys124-Cys169 and Cys168-177 were identified as a double SS bond in IB.[19] These SS bonds were found to provide stability to local structure and dynamics.

Structural Changes

To investigate structural changes in the proteins, vector analysis was used to track coordinates of the center of mass of each protein domain, relative to the origin, over the entire trajectory of all simulation runs. Separation distances (Euclidean distance) between domains over time were then calculated using the coordinates. In IgG, vector coordinates of the center of mass of the $F_{ab}1$, $F_{ab}2$, and F_c domains were calculated. In BSA, vector coordinates of the center of mass of the I, II, and III domains were calculated. Pairwise separation distances were computed. After vector analysis, VMD was used visualize conformational changes in IgG and BSA after cleavage of SS bonds. For reference, **Figure 10** shows a visualization of IgG and BSA with their respective domain centers of mass highlighted and associated distances displayed.

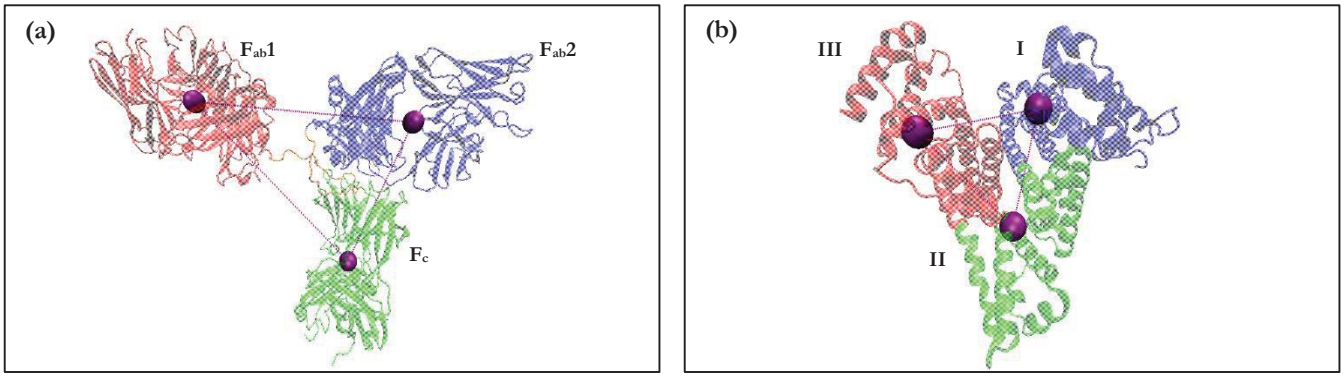

Figure 10. Cartoon representation of IgG (a) depicts centers of mass as purple van der Waals (vdW) spheres and associated distances as dashed purple lines. Regions are represented as: $F_{ab}1$ (red), $F_{ab}2$ (blue), F_c (green), and hinge (orange). Cartoon representation of BSA (b) depicts centers of mass as purple van der Waals (vdW) spheres and associated distances as dashed purple lines. Domains are represented as: I (blue), II (green), and III (red). The cartoons were created using Visual Molecular Dynamics.[26]

Distances between domains $F_{ab}1$ and F_c, as well as between $F_{ab}2$ and F_c, remained stable across all simulation runs (1-3), with little deviation between IgG systems. **Figure 11** details a notable observation in the distance between the centers of mass for $F_{ab}1$ and $F_{ab}2$. For simulation runs 1 and 3, the distances between the two domains remained stable over evolution of 200 ns with average

values of 81.5±2.25 Å and 79.9±2.36 Å, respectively. The separation distance in simulation run 2 maintained an average value of 75.6±4.94 Å during the entire simulation time. The distance increased for the first ~15 ns, then decreased significantly for ~45 ns, where the distance then remained at a stable 72.2±1.26 Å for ~20 ns, and then increased again to remain at a stable 73.8±1.24 Å for the remainder of simulation time. After ~30 ns, the separation distance between the two domains for simulation run 2 was consistently lower than those for simulation runs 1 and 3, suggesting a contraction of the protein structure. Separation distances in simulation runs 1 and 3 were not significantly different (deviation of average values for equivalent sample sizes overlapped), indicating that removal of the Cys236H-Cys236K SS bond was not responsible for the contraction.

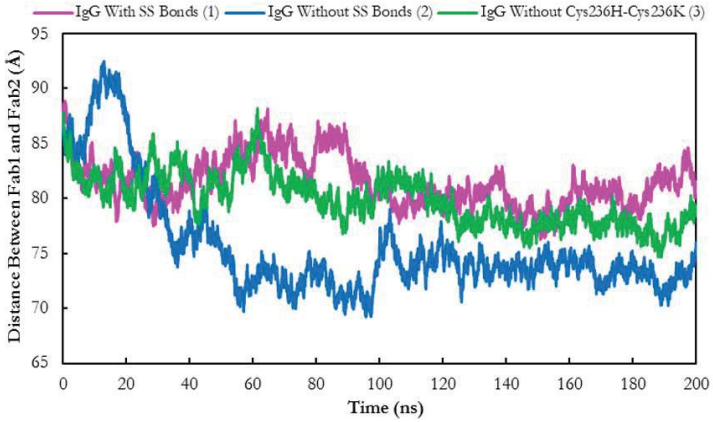

Figure 11. Distance between centers of mass of $F_{ab}1$ and $F_{ab}2$ domains for IgG simulations 1-3. Distances are presented for IgG with SS Bonds (simulation run 1, pink), IgG without SS Bonds (simulation run 2, blue), and IgG without Cys236H-Cys236K (simulation run 3, green).

Vector analysis of IgG was followed by use of VMD to visualize structural changes. The hinge region itself lacks secondary structure; therefore, absence of stabilizing forces allows for the perceived segmental motion and flexibility. With this knowledge, visualization of local structure about the hinge region would not provide relevant observations. Visualization of domains displayed evidence of the contraction seen in **Figure 11**. **Figure 12** shows snapshots of IgG during simulation run 2 (without SS bonds) at 20 ns (**Figure 12a**) and at 120 ns (**Figure 12b**). Relative to the protein structure in early stages of the trajectory, distance between $F_{ab}1$ and $F_{ab}2$ domains of IgG decreased. This contraction was seen in the IgG molecule, and this state persisted for the remainder of simulation time. When trajectories of simulation run 1 and 3 (with SS bonds and without Cys236H-Cys236K) were visualized, no similar contraction was seen. Again, this suggested that cleavage of Cys236H-Cys236K was not directly responsible for the observed conformational change.

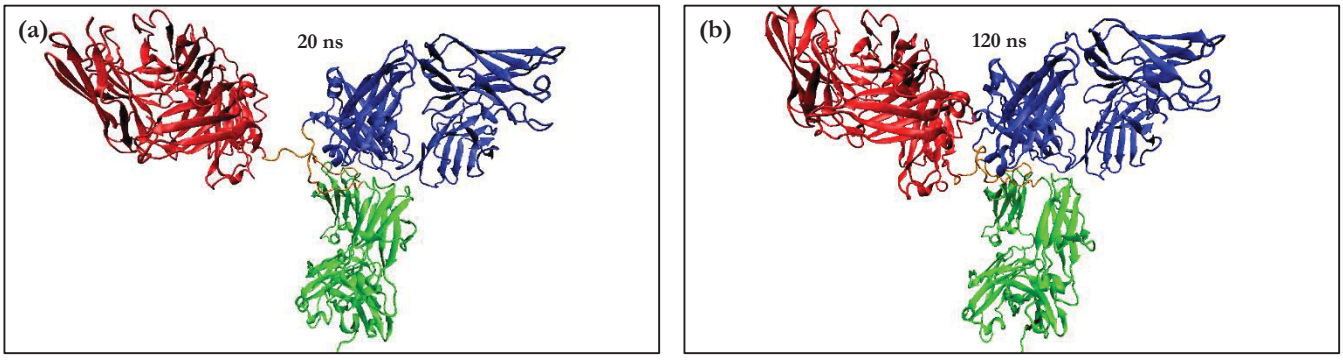

Figure 12. Cartoon representation of IgG at 20 ns (a) and 120 ns (b). Regions are represented as: $F_{ab}1$ (red), $F_{ab}2$ (blue), F_c (green), and hinge (orange). Contraction of protein is seen with the decrease in distance between $F_{ab}1$ and $F_{ab}2$ domains. The cartoons were created using Visual Molecular Dynamics.[26]

In BSA, pairwise distances between domains I, II, and III were computed. Distances remained stable across all simulations runs (4-8), with little deviation between BSA systems. **Figure 13** shows distances for domains I-II, I-III, and II-III over 200 ns simulation time. Domains I and II maintained an average distance of 32±0.4 Å, and domains I and III had an average distance of 35±0.7 Å for all simulation runs. For domains II and III, distances fluctuated around 35±0.6 Å. In all cases, distances were not significantly different across simulation runs.

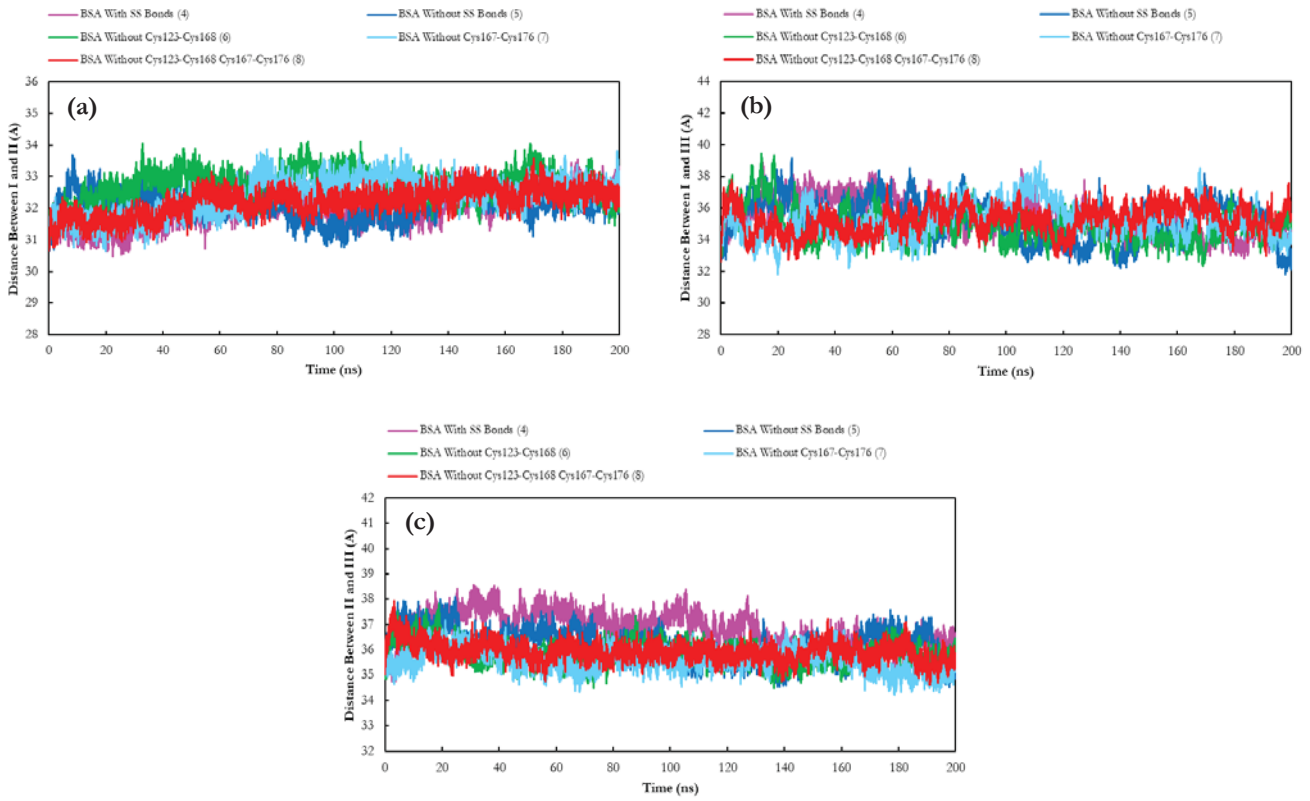

Figure 13. Distance between centers of mass of I, II, and III domains for BSA simulations 4-8. Distances for I-II (a), I-III (b), and II-III (c) are presented for BSA with SS Bonds (simulation run 4, in pink), without SS Bonds (simulation run 5, in blue), without Cys123-Cys168 (simulation run 6, in green), without Cys167-Cys176 (simulation run 7, in teal), and without Cys123-Cys168 and Cys167-Cys176 (simulation run 8, in red).

All SS bonds of BSA are buried in the α helices of the protein structure. The protein's globular nature imparts little to no flexibility. Therefore, large deviations in distances between domains of BSA were not expected. Upon application of the prescreening method, Sγ atom pairs of the double SS bond (Cys123-Cys168 and Cys167-Cys176) of BSA with all SS bonds cleaved separated significantly; this suggested possible changes in local protein structure. Three α helices were involved in the double SS bond. These helices, identified as A, B, and C, were comprised of residues 119-145, residues 150-172, and residues 175 to 195, respectively. Cys123-Cys168 was between helices A and B, and Cys167-Cys176 was between helices B and C. **Figure 14** shows snapshots of those α helices in BSA during simulation run 5 (without SS bonds) at 10 ns (**Figure 14a**) and 180 ns (**Figure 14b**). A local perturbation in secondary structure was seen in helix C during the course of the simulation run, as identified in the figure.

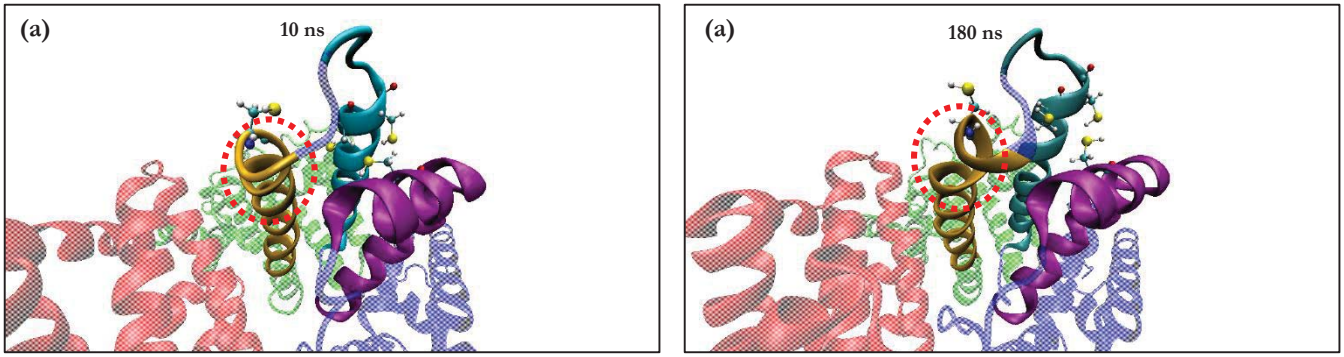

Figure 14. Cartoon representation of BSA at 10 ns (a) and 180 ns (b). Domains are represented as: I (blue), II (green), and III (red). Helices are represented as: A (purple), B (cyan), and C (orange). SS bonds are represented as ball-and-stick. Local perturbation in secondary structure seen in helix C, as identified by the red circle. The cartoons were created using Visual Molecular Dynamics.[26]

Because of the distinct protein structures of IgG and BSA, the role and contributions of SS bonds to overall structure maintenance were inherently dissimilar. As discussed, application of the prescreening methodology showed that Sγ atom pairs of inter-chain SS bonds in IgG deviated significantly, while pairs in intra-chain SS bonds did not. Unlike intra-chain SS bonds, inter-chain bonds of IgG are not buried in β sheets; therefore, secondary structure cannot supplement interactions in these local residues. Specifically, the selected SS bond for cleavage, Cys236H-Cys236K, was between two heavy chains in the hinge region. Thus, analysis of structural change in IgG was made at the domain level, and a contraction of the protein was observed. In contrast, all SS bonds of BSA are intra-domain and buried in α helices. For Sγ atom pairs with significant deviations, secondary structure was present, but did not stabilize local interactions. This suggested more local structural changes, and perturbations were observed at the α helix level. In the case of IgG, the selected SS bond (Cys236H-Cys236K) did not reproduce the contraction, but separation distance data does suggest that one or more of the three inter-chain SS bonds contributed to structural changes in simulation run 2 (without SS bonds). In both cases, the prescreening method showed that analyzing simulations of proteins with all native SS bonds cleaved and calculating Sγ atom pair separation distances successfully identified specific SS bonds critical to structural stability.

CONCLUSIONS

In this study, a prescreening methodology introduced in previous work by our lab to identify potentially significant SS bonds was extended to study their role in the stabilization of IgG and BSA. IgG was selected for its importance in current monoclonal antibody therapies, high density of SS bonds, and novel structure. BSA maintains structural homology with HSA, the protein studied in our previous work, and therefore provided an avenue through which the relationship between structure and function could be considered. Atomistic MD simulations of IgG and BSA were performed for a total simulation time of 1.6 μs. For each protein, SS bond distances for independent simulation runs with native SS bonds cleaved were calculated and analyzed. The relative importance of inter, intra, and double SS bonds was evaluated with respect to which sulfur atom pairs deviated significantly from the average disulfide bond distance (2.05 Å).

In IgG, RMSD analyses of three independent simulation runs showed longer equilibration time scales for runs without all native SS bonds, indicating the likelihood of structural changes. Only Sγ atoms of inter-chain SS bonds, such as Cys236H-Cys236K, showed significant (>6 Å) deviations in distances, while those of intra-chain SS bonds remained in a stable range of 3 to 6 Å. The high degree of β sheet secondary structure likely stabilized intra-chain SS bonds. Thus, intra-chain SS bonds of IgG may provide redundant interactions for conformational stability or play a role in protein function. Vector analysis and visualization showed a contraction of the protein between $F_{ab}1$ and $F_{ab}2$ domains, but cleavage of only Cys236H-Cys236K showed it was not solely responsible. This does not discount the possibility of one or more inter-chain SS bonds contributing to these protein dynamics. In BSA, all SS bonds are intra-domain and supplemented by secondary structure of α helices. Sγ atoms of several bonds, including a double SS bond (Cys123-Cys168 and Cys167-Cys176), showed significant deviations. Previous work on HSA showed a homologous double SS bond, whose Sγ atoms also deviated significantly upon cleavage and contributed to structural stability. Analysis and visualization showed that Cys167-Cys176 may noticeably contribute to maintaining local structure.

This work demonstrated the efficacy of a previously established prescreening methodology in the use of atomistic simulations to identify structurally significant SS bonds. In simulations of both IgG, a large, Y-shaped protein, and BSA, a small, globular protein similar to HSA, use of the methodology effectively identified pairs of Sγ atoms with significant changes in distances. Application of the prescreening method was achieved; future work may include more rigorous analysis of protein dynamics shown in this study (local RMSDs, secondary structure analysis, correlated motions, etc.). The absence of select disulfide bonds in proteins has been identified to lead to susceptibility to protein aggregation. These simulations provide information on the effects of specific SS bonds in conformational stability of both proteins, and the discussed method provides a predictive power in identifying these bonds, which may be critical in protein stability and/or aggregation phenomena. Additionally, prediction of SS bonds relevant to protein stabilization can be subsequently tested experimentally (selective reduction), providing a practical approach for faster screening in SS bond analysis. Results of this prompt more comprehensive insight into the role of SS bonds and changes in protein dynamics following their absence.

ACKNOWLEDGEMENTS

The authors thank Dr. Ping Lin and Dr. Maria Monica Castellanos for assistance in the modeling and reconstruction of the IgG structure. They also acknowledge the computational resources (HiPerGator 2.0) provided by University of Florida Research Computing and the funding provided by National Science Foundation (grant ACI-1613155).

REFERENCES

1. Berg, J. M., Tymoczko, J. L., and Stryer, L. (2002) *Biochemistry* 5th ed., 84–137, W. H. Freeman, New York.

2. Bulaj, G. (2005) Formation of disulfide bonds in proteins and peptides, *Biotechnol. Adv.* 23, 87–92. doi:10.1016/j.biotechadv.2004.09.002.

3. Trivedi, M. V., Laurence, J. S., and Siahaan, T. J. (2009) The role of thiols and disulfides in protein chemical and physical stability, *Curr. Protein Pept. Sci.* 10(6), 614–625. doi:10.2174/138920309789630534.

4. Creighton T. E. (1997) Protein folding coupled to disulphide bond formation, *Biol. Chem.* 378(8), 731–744. doi:10.1515/bchm.1997.378.8.731.

5. Ross, C. A., and Poirier, M. A. (2004) Protein aggregation and neurodegenerative disease, *Nat. Med.* 10, S10–S17. doi:10.1038/nm1066.

6. Trottier Y., Lutz Y., Stevanin G., Imbert G., Devys D., Cancel G., Saudou F., Weber C., David G., Tora L., Agid Y., Brice A., and Mandel J. L. (1995) Polyglutamine expansion as a pathological epitope in Huntington's disease and four dominant cerebellar ataxias, *Nature* 378, 403–406. doi:10.1038/378403a0.

7. Voisine C., Pedersen J. S., and Morimoto R. I. (2010) Chaperone networks: Tipping the balance in protein folding diseases, *Neurobiol. Dis.* 40(1), 12–20. doi:10.1016/j.nbd.2010.05.00.

8. Williams A., Jahreiss L., Sarkar S., Saiki S., Menzies F. M., Ravikumar B., and Rubinsztein D. C. (2006) Aggregate-prone proteins are cleared from the cytosol by autophagy: Therapeutic implications, *Curr. Top. Dev. Biol.* 76, 89–101. doi:10.1016/S0070-2153(06)76003-3.

9. Cho S. S., Levy Y., Onuchic J. N., and Wolynes P. G. (2005) Overcoming residual frustration in domain-swapping: the roles of disulfide bonds in dimerization and aggregation, *Phys. Biol.* 2, S44–S55. doi:10.1088/1478-3975/2/2/S05.

10. Welker E., Wedemeyer W. J., and Scheraga H. A. (2001) A role for intermolecular disulfide bonds in prion diseases? *Proc. Natl. Acad. Sci. USA* 98, 4334–4336. doi:10.1073/pnas.071066598.

11. Liu, H., and May, K. (2012) Disulfide bond structures of IgG molecules: Structural variations, chemical modifications and possible impacts to stability and biological function, *MAbs.* 4(1), 17–23. doi:10.4161/mabs.4.1.18347.

12. Yang, M., Dutta, C., and Tiwari, A. (2015) Disulfide-bond scrambling promotes amorphous aggregates in lysozyme and bovine serum albumin, *J. Phys. Chem. B* 119(10), 3969–3981. doi:10.1021/acs.jpcb.5b00144.

13. Betz, S. F. (1993) Disulfide bonds and the stability of globular proteins, *Protein Sci.* 2(10), 1551–1558. doi:10.1002/pro.5560021002.

14. Borges, C. R., and Sherma, N. D. (2014) Techniques for the analysis of cysteine sulfhydryls and oxidative protein folding, *Antioxid. Redox Signal.* 21(3), 511–531. doi:10.1089/ars.2013.5559.

15. Buyong M. A., Xiong, J., Lubkowski, J., and Nussinov, R. (2000) Homology modeling and molecular dynamics simulations of lymphotactin, *Protein Sci.* 9(11), 2192–2199. doi:10.1110/ps.9.11.2192.

16. Godwin, A., Choi, J. W., Pedone, E. et al. (2007) Molecular dynamics simulations of proteins with chemically modified disulfide bonds, *Theor. Chem. Acc.* 117, 259. doi:10.1007/s00214-006-0134-0.

17. He J., Xu L., Zou Z., Ueyama N., Li H., Kato A., Jones G. W., and Song Y. (2013) Molecular dynamics simulation to investigate the impact of disulfide bond formation on conformational stability of chicken cystatin I66Q mutant, *J Biomol. Struct. Dyn.* 31(10), 1101–1110. doi:10.1080/07391102.2012.721498.

18. Zhang, L. (2017) Different dynamics and pathway of disulfide bonds reduction of two human defensins, a molecular dynamics simulation study, *Proteins Struct. Funct. Bioinf.* 85(4), 665–681. doi:10.1002/prot.25247.

19. Castellanos, M. M., and Colina, C. M. (2013) Molecular dynamics simulations of human serum albumin and role of disulfide bonds, *J. Phys. Chem. B* 117 (40), 11895–11905. doi:10.1021/jp402994r.

20. Vidarsson, G., Dekkers, G., and Rispens, T. (2014) IgG subclasses and allotypes: From structure to effector functions, *Front. Immunol.* 5, 520. doi:10.3389/fimmu.2014.00520.

21. Sandin, S., Ofverstedt, L. G., Wikstrom, A. C., Wrange, O., and Skoglund, U. (2004) Structure and flexibility of individual immunoglobulin G molecules in solution, *Structure* 12, 409–415. doi:10.1016/j.str.2004.02.011.

22. Berman, H. M., Westbrook, J., Feng, Z., Gilliland, G., Bhat, T. N., Weissig, H., Shindyalov, I. N., and Bourne, P. E. (2000) The Protein Data Bank, *Nucleic Acids Res.* 28, 235–242.

23. Saphire, E., Parren, P., Pantophlet, R., Zwick, M., Morris, G., Rudd, P., Dwek, R., Stanfield, R., Burton, D., and Wilson, I. (2001) Crystal structure of a neutralizing human IGG against HIV-1: a template for vaccine design, *Science* 293, 1155–1159. doi:10.1126/science.1061692.

24. Chames, P., Van R. M., Weiss, E., and Baty, D. (2009) Therapeutic antibodies: successes, limitations and hopes for the future, *Br. J. Pharmacol.* 157(2), 220–233. doi:10.1111/j.1476-5381.2009.00190.x.

25. Michaelsen, T. E., Brekke, O. H., Aase, A., Sandin, R. H., Bremnes, B., and Sandlie, I. (1994) One disulfide bond in front of the second heavy chain constant region is necessary and sufficient for effector functions of human IgG3 without a genetic hinge, *Proc. Natl. Acad. Sci. USA* 91(20), 9243–9247.

26. Humphrey, W., Dalke, A., and Schulten, K. (1996) VMD: Visual Molecular Dynamics, *J. Molec. Graphics* 14, 33−38. doi:10.1016/0263-7855(96)00018-5.

27. Merlot A. M., Kalinowski D. S., and Richardson D. R. (2014) Unraveling the mysteries of serum albumin—more than just a serum protein, *Front. Physiol.* 5, 299. doi:10.3389/fphys.2014.00299.

28. Gelamo E. L., and Tabak M. (2000) Spectroscopic studies on the interaction of bovine (BSA) and human (HSA) serum albumins with ionic surfactants, *Spectrochim. Acta A Mol. Biomol. Spectrosc.* 56, 2255–2271. doi:10.1016/S1386-1425(00)00313-9.

29. Majorek, K. A., Porebski, P. J., Dayal, A., Zimmerman, M. D., Jablonska, K., Stewart, A. J., and Minor, W. (2012) Structural and immunologic characterization of bovine, horse, and rabbit serum albumins, *Mol. Immunol. 52*(3-4), 174–182. doi:10.1016/j.molimm.2012.05.011.

30. Sugio, S., Kashima, A., Mochizuki, S., Noda, M., and Kobayashi, K. (1999) Crystal structure of human serum albumin at 2.5 Å resolution, *Protein Eng.* 12, 439−446. doi:10.1093/protein/12.6.439.

31. Case, D. A., Betz, R. M., Cerutti, D. S., Cheatham, T. E., III, Darden, T. A., Duke, R. E., Giese, T. J., Gohlke, H., Goetz, A. W., Homeyer, N., Izadi, S., Janowski, P., Kaus, J., Kovalenko, A., Lee, T. S., LeGrand, S., Li, P., Lin, C., Luchko, T., Luo, R., Madej, B., Mermelstein, D., Merz, K. M., Monard, G., Nguyen, H., Nguyen, H. T., Omelyan, I., Onufriev, A., Roe, D. R., Roitberg, A., Sagui, C., Simmerling, C. L., Botello-Smith, W. M., Swails, J., Walker, R. C., Wang, J., Wolf, R. M., Wu, X., Xiao, L. and Kollman, P. A. (2016) AMBER 2016, University of California, San Francisco.

32. Salomon-Ferrer, R., Goetz, A., Poole, D., Le Grand, S., and Walker, R. (2013) Routine microsecond molecular dynamics simulations with AMBER on GPUs. 2. explicit solvent particle mesh Ewald, *J. Chem. Theory Comput.* 9, 3878–3888. doi:10.1021/ct400314y.

33. Maier, J. A., Martinez, C., Kasavajhala, K., Wickstrom, L., Hauser, K. E., and Simmerling, C. (2015) ff14SB: Improving the accuracy of protein side chain and backbone Pparameters from ff99SB, *J. Chem. Theor. Comput.* 11, 3696–3713. doi:10.1021/acs.jctc.5b00255.

34. Jorgensen, W. L., Chandrasekhar J., Madura J. D., Impey R. W., and Klein, M.L. (1983) Comparison of simple potential functions for simulating liquid water, *J. Chem. Phys.* 79, 926. doi:10.1063/1.445869.

35. Mahoney, M. W., and Jorgensen, W. L. (2000) A five-site model liquid water and the reproduction of the density anomaly by rigid, non-polarizable models, *J. Chem. Phys. 112*, 8910–8922. doi:10.1063/1.481505.

36. Crowley, M., Darden, T., Cheatham, T., III, and Deerfield, D., II. (1997) Adventures in improving the scaling and accuracy of a parallel molecular dynamics program, *J. Supercomput.* 11, 255–278. doi:10.1023/A:1007907925007.

37. Darden, T., York, D., Pedersen, L. (1993) Particle mesh ewald: An N ·log(N) method for ewald sums in large systems, *J. Chem. Phys.* 98, 10089–10092. doi:10.1063/1.464397.

38. Essmann, U., Perera, L., Berkowitz, M. L., Darden, T., Lee, H., and Pedersen, L. G. (1995) A smooth particle mesh ewald method, *J. Chem. Phys.* 103, 8577–8593. doi:10.1063/1.470117.

39. Roe, D. R., Cheatham, T. III. (2013) PTRAJ and CPPTRAJ: Software for processing and analysis of molecular dynamics trajectory data*, J. Chem. Theory Comput.* 9, 3084–3095. doi:10.1021/ct400341p.

40. Fortunato, M. E., and Colina, C. M. (2014) Effects of galactosylation in immunoglobulin G from all-atom molecular dynamics simulations, *J. Phys. Chem. B* 118 (33), 9844–9851. doi:10.1021/jp504243e.

41. Bošnjak, I., Bojović, V., Šegvić-Bubić T., Bielen, A. (2014) Occurrence of protein disulfide bonds in different domains of life: a comparison of proteins from the Protein Data Bank, *Protein Eng. Des. Sel.* 27 (3), 65–72. doi.org/10.1093/protein/gzt063.

ABOUT THE STUDENT AUTHORS

Akshay Mathavan grew up in Davie in South Florida. He is currently an undergraduate junior student at the University of Florida, where he is pursuing a B. S. in Biomedical Engineering with minors in Mathematics and Computer Science. Akshay joined the Colina Research Group in the Winter of 2016. He plans to attend medical school and become an oncologist.

Akash Mathavan joined the Colina Research Group in December 2016. He grew up in Davie, Florida. Currently an undergraduate junior at the University of Florida, he is pursuing a B. S. in Biomedical Engineering with minors in Mathematics and Computer Science. He is interested in attending medical school and engaging in surgery.

Mike Fortunato earned his B. S. and M.S. in Materials Science and Engineering at the Pennsylvania State University in 2012 and 2015. He joined the Colina Research Group at the University of Florida in 2015 and is a Ph.D. candidate.

PRESS SUMMARY

Research indicates that disulfide bonds may play an important role in the stabilization of protein structure and conformation. In this study, atomistic molecular dynamics simulations were performed on Immunoglobulin G and Bovine Serum Albumin. A previously established prescreening methodology was extended to both proteins to identify disulfide bonds with significant contributions to local structure, supporting the reproducibility of the methodology. The prescreening methodology can therefore be applied as a predictive tool to gauge the relative importance of disulfide bonds to structural stability, which can then be experimentally tested. This work provides insight into the role of these specific disulfide bonds in the stabilization of protein structure.